Journal of Sound and Vibration 328 (2009) 488–506

Contents lists available at ScienceDirect

Journal of Sound and Vibration

journal homepage: www.elsevier.com/locate/jsvi

Characterization and reduction of dynamic models of vibrating systems with high modal density

Jean-Louis Guyader *

Laboratoire Vibrations- Acoustique, Institut National des Sciences Appliquées de Lyon, 69621 Villeurbanne, France

ARTICLE INFO

Article history:
Received 21 December 2007
Received in revised form
29 July 2009
Accepted 5 August 2009
Handling Editor: C.L. Morfey
Available online 1 October 2009

ABSTRACT

The aim of this paper is to demonstrate that the vibration response of systems with high modal density excited by broadband forces can be obtained by decomposing the response on a small number of effective shapes instead of a large number of mode shapes. An approach for building effective shapes on the basis of a measured mobility matrix is presented. More precisely, effective shapes can be built from eigenvectors of the space-frequency mobility matrix and a reduced model can be obtained by using only a small number of dominant eigenvectors of the SFM matrix. Systems with high modal density are characteristic of mid and high frequency problems where, for the sake of robustness, energy is often preferred to local response in order to describe the behavior of vibrating systems. The models built from the eigenvectors of the SFM matrix can be used for energy prediction and we observe that very small models are sufficient for prediction to within 3 dB. Two applications of the method are presented: the first uses numerical results in the case of longitudinal beam vibrations while the second uses experimental results obtained from plate vibrations. The method is in fact an extension of experimental modal analysis to the vibration problems of systems with high modal density.

1. Introduction

In noise and vibration control, dynamic models of structures are vital tools for ensuring better acoustic quality. When an existing structure must be improved, a model can be built by using experimental data for predicting structural responses to modified excitations, additional excitations (active control) and after coupling with other structures.

Building models with experimental data is a well-known problem in structural dynamics and the basic approach used is modal analysis which consists in identifying the modes controlling the response. A great deal of literature on this topic exists and we do not intend to present it here, however the reader can refer to Ref. [1] for more information. The standard technique is to measure the frequency response function (FRF) to extract modal information. In several mechanical applications, high spatial resolution frequency responses are measured with a laser vibrometer, resulting in a large amount of data. However, the data set obtained is corrupted by measurement noise. Thus one major hurdle to be overcome is that of reducing the amount of data in order to conserve only the information associated with the few modes controlling the response and, consequently, avoid noise. The singular value decomposition (SVD) technique is perfectly adapted to this task of data reduction and this method has recently been presented in several papers [2–4].

* Tel.: +33 472 43 80 80; fax: +33 472 43 87 12.
E-mail address: Jean-louis.guyader@insa-lyon.fr

0022-460X/$ - see front matter © 2009 Elsevier Ltd. All rights reserved.
doi:10.1016/j.jsv.2009.08.012

Modal analysis is adapted to the description of vibration behavior involving only a few modes, but it is not appropriate when the number of modes participating in the response increases as in medium or high frequency vibro-acoustic problems. In this case, it is possible to use FRF data and the mobility concept, for coupling substructures directly, see for example [5]. As in the case of previous articles, this one uses FRF data for structure characterization. However, instead of using FRF directly, it aims to demonstrate that in the case of a high number of modes participating in the motion, it is possible to express the response by gathering these modes in a much smaller number of effective shapes calculated from the measured FRF. The advantage of a description with effective shapes lies in their physical meaning, comparable for medium frequency to mode shapes at low frequency. Thus indication through the use of effective shapes of structural zones of high and low vibration amplitude is physically important to control the excitation of the structure. In the case of active control with secondary sources, the effective shapes of high eigenvalues are the motions that have to be eliminated to reduce vibrations. Statistical energy analysis (SEA) makes it possible to group modes for problems in which a very large number of modes respond. This method assumes that all the resonant modes of a subsystem have the same energy (energy equipartition). A large number of papers have already dealt with SEA and it is not the purpose of this paper to give a general presentation of the method, rather it gives a simple overview. The basis of SEA was derived by Lyon and Maidanik [6], after which Lyon [7] and Lyon and DeJong [8] provided a synthetic presentation. Much work was done on estimating coupling loss factors (C.L.F.) to characterize the coupling of two groups of modes. Langley [9] presented a based wave method for deriving C.L.F., Bies and Hamid [10] applied an inverse technique to identify C.L.F., and Maxit and Guyader [11] used Karnopp's dual formulation [12] to calculate C.L.F. from inter-modal work. Discussion on the basic SEA model (Mace and Rosenberg [13], Finnveden [14]), as well as the extension of the method when energy equipartition is not achieved (Maxit and Guyader [15]), have been proposed. Finally, Totaro and Guyader presented an automatic partitioning technique [16].

From these papers one can conclude that at medium and high frequencies where a great many modes respond, one way of ensuring the appropriate decomposition of the response is to group modes rather than by treating them independently. The goal of this paper is to explain how grouping modes in effective shapes can be done by using the space frequency mobility matrix (SFM matrix). The SFM matrix describes the velocity of receiving points at different frequencies in a band, when the structure is driven by a harmonic point force of unit amplitude. Each term of the SFM matrix can be interpreted as a transfer mobility. The mobility concept is widely used in structural vibrations for source characterization and sub-structuring techniques [17–23]. More recently, the mobility approach has been extended to vibroacoustic coupling [24] and energy coupling [25]. Thus the experimental technique required to obtain SFM matrices has been well established and measurements can be extended to vibroacoustic problems.

Square SFM matrices are considered in the following in order to use powerful linear algebra theorems, resulting in a simple explanation of the physics underlying mode grouping. Measured SFM matrices are generally rectangular in medium frequency problems, because the number of frequency points is higher than the number of space points. However, it is straightforward to use the present method for rectangular matrices by adding columns of zeros to obtain a square matrix, as explained in this paper.

An important property of the SFM matrix described in this paper is associated with its dominant eigenvalues. The corresponding eigenvectors constitute a set of effective shapes that form a basis for decomposing the response. These eigenvalues and eigenvectors are linked to the modes controlling the response but are not the modes.

A result of mode grouping is that the response can be well-approximated by decomposition on a small number of eigenvectors (effective shapes) resulting in a reduced dynamic model. Obviously, dynamic model reduction methods have already been proposed, in particular both Soize [26] and Ohayon [27] considered vibroacoustic problems, Ghanem and Sarkar [28] treated stochastic systems and Guyader [29] proposed a modal sampling technique. However, the present approach is clearly oriented towards an experimental application, since the reduced model is constructed from measured data.

2. Definition of space-frequency mobility

A linear vibrating system is driven at point x_i by the harmonic excitation of angular frequency ω_k and unit amplitude. The velocity response at point x_j takes the form (1):

$$W^i(x_j,\omega_k)\exp(\mathrm{j}\omega_k t) \tag{1}$$

Responses at several points x_j for angular frequencies varying in a band according to Eq. (2) are considered.

$$\omega_k = \Omega_{\min} + k\Delta, k = 0, N-1 \tag{2}$$

where Δ is the angular frequency step.

The space-frequency mobility (SFM) matrix, denoted matrix $\mathbf{G}^i$ in the following, defined in Eq. (3), characterizes the response of the system at all points x_j and angular frequency ω_k, when it is excited at point x_i:

$$\mathbf{G}^i = [g^i(j,k)] = [W^i(x_j,\omega_k)] \tag{3}$$

For the sake of simplicity, a square matrix is considered here whereas the case of a rectangular matrix is studied in Section 5.

The response at point x_j when the excitation is located at point x_i and takes form (4), can be calculated with the SFM matrix, as demonstrated in Eq. (5).

$$F^i(t) = \sum_{k=0}^{N-1} A_k^i \exp(\mathrm{j}\omega_k t) \tag{4}$$

$$W^i(x_j, t) = \sum_{k=0}^{N-1} g^i(j,k) A_k^i \exp(\mathrm{j}\omega_k t) \tag{5}$$

In Eqs. (4) and (5), the discretized form of the Fourier integral is used to express the force and displacement in the time domain. In matrix form Eq. (5) is written as:

$$\mathbf{w}^i(t) = \mathbf{G}^i \mathbf{f}^i(t) \tag{6}$$

where the driving force and displacement vectors are:

$$\mathbf{f}^i(t) = \{A_k^i \exp(\mathrm{j}\omega_k t)\} \mathbf{w}^i(t) = \{W^i(X_j, t)\} \tag{7}$$

Vibration time history can be obtained by using Eq. (6) at each instant to calculate the displacements from the applied force.

3. Fundamental property of the SFM matrix

3.1. Two matrix properties

In this section two well known properties of matrices are recalled as they are of interest for the following.

1. The rank of a matrix equal to the product of 2 matrices, obeys Eq. (8):

$$\mathrm{rank}(AB) \leq \sup(\mathrm{rank(A)}, \mathrm{rank(B)}) \tag{8}$$

2. The number of non nil eigenvalues of a matrix is equal to its rank and the product of the matrix by any vector remains in a subspace. The eigenvectors associated with non nil eigenvalues constitute a basis of this subspace.

3.2. Case of one mode controlling the response

To establish the fundamental property of matrix $\mathbf{G}^i$ we initially consider that the vibration of the system under study is described by one mode. Thus the vibratory response is given by Eq. (9):

$$W^i(x_j, \omega_k)\exp(\mathrm{j}\omega_k t) = H_\alpha(\omega_k)\varphi_\alpha(x_j)\varphi_\alpha(x_i)A_k^i \exp(\mathrm{j}\omega_k t) \tag{9}$$

where

$$H_\alpha(\omega_k) = \frac{\mathrm{j}\omega_k}{(\Omega_\alpha^2 - \omega_k^2 + 2\mathrm{j}\varepsilon_\alpha \Omega_\alpha \omega_k) M_\alpha}$$

is the mode frequency response, Ω_α is the normal angular frequency of the mode, M_α the modal mass and ε_α the damping coefficient and $\varphi_\alpha(x_i)$ is the mode shape at point x_i.

In this case matrix G^i has a simple form (10):

$$\mathbf{G}^i = \begin{bmatrix} H_\alpha(\omega_1)\varphi_\alpha(x_1)\varphi_\alpha(x_i) & \dots & \dots & \dots & H_\alpha(\omega_N)\varphi_\alpha(x_1)\varphi_\alpha(x_i) \\ \vdots & & & & \vdots \\ \vdots & & & & \vdots \\ \vdots & & & & \vdots \\ H_\alpha(\omega_1)\varphi_\alpha(x_N)\varphi_\alpha(x_i) & & & & H_\alpha(\omega_N)\varphi_\alpha(x_N)\varphi_\alpha(x_i) \end{bmatrix} \tag{10}$$

It is possible to decompose matrix $\mathbf{G}^i$ into a product of 2 matrices:

$$\mathbf{G}^i = \mathbf{\Phi}\mathbf{H}^t \tag{11}$$

Where

$$\mathbf{H} = \begin{bmatrix} H_\alpha(\omega_1) \\ \vdots \\ \vdots \\ \vdots \\ H_\alpha(\omega_N) \end{bmatrix} \quad \text{and} \quad \mathbf{\Phi} = \begin{bmatrix} \varphi_\alpha(x_1)\varphi_\alpha(x_i) \\ \vdots \\ \vdots \\ \vdots \\ \varphi_\alpha(x_N)\varphi_\alpha(x_i) \end{bmatrix}$$

are single column matrices of the mode frequency responses at the different excited angular frequencies and of the product of mode shapes at the excitation point and all the observation points, while $\mathbf{H}^t$ is the matrix transpose of $\mathbf{H}$.

Single column matrices or single row matrices have a rank equal to or less than 1; in addition, the rank of a matrix equal to the product of 2 matrices obeys Eq. (8). It can be concluded that the rank of the SFM matrix is equal to 1 or to 0 when one mode controls the response.

The application of the above in the case presented here establishes the basic property of the SFM matrix when the response is controlled by one mode:

- The number of non nil eigenvalues is equal to 1 or to 0.
- The response to any excitation vector is proportional to the eigenvector of the non nil eigenvalue.

To clarify the property, let us calculate the product of the SFM matrix by a vector $\mathbf{v}$ by using Eq. (10). This leads to Eq. (12):

$$\mathbf{G}^i\mathbf{v} = \mathbf{\Phi}\mathbf{H}^t\mathbf{v} = a\mathbf{\Phi} \tag{12}$$

where $a = \mathbf{H}^t\mathbf{v}$ is a scalar value.

If $\mathbf{v} = \mathbf{\Phi}$ is chosen the previous result is written as:

$$\mathbf{G}^i\mathbf{\Phi} = \lambda\mathbf{\Phi} \tag{13}$$

where $\lambda = \mathbf{H}^t\mathbf{\Phi}$ appears as the eigenvalue of the SFM matrix and the single column matrix $\mathbf{\Phi}$ is the associated eigenvector. The eigenvalue can be calculated, providing:

$$\lambda = \sum_{k=1}^{N} H_\alpha(\omega_k)\varphi_\alpha(x_k)\varphi_\alpha(x_i) \tag{14}$$

It is clear from Eq. (14) that the eigenvalue is nil if the excitation point is located on a node or if all the measurement points are located on nodes. Generally, the second situation is not observed although the first one can be encountered. When the previous case is not satisfied, the eigenvalue is different from 0. In addition, it has a high value if the mode has a marked frequency response in the excited band; this is the case of lightly damped resonant modes, as $H_\alpha(\omega_k)$ has high values in the excited band. It should be added that the eigenvalue also depends on the number of space points considered, as can be seen in Eq. (14).

3.3. Case of 2 modes controlling the response

3.3.1. Rank of the SFM matrix

In this case the vibratory response takes the form:

$$W^i(x_j,\omega_k)\exp(\mathrm{j}\omega_k t) = (H_\alpha(\omega_k)\varphi_\alpha(x_j)\varphi_\alpha(x_i) + H_\beta(\omega_k)\varphi_\beta(x_j)\varphi_\beta(x_i))A_k^i\exp(\mathrm{j}\omega_k t)$$

It is straightforward to demonstrate that:

$$\mathbf{G}^i = \mathbf{\Phi}\mathbf{H}^t \tag{15}$$

where $\mathbf{H} = [\mathbf{h}_\alpha\ \mathbf{h}_\beta]$ is a matrix with two columns where:

$$\mathbf{h}_\alpha = \begin{Bmatrix} H_\alpha(\omega_1) \\ \vdots \\ \vdots \\ \vdots \\ H_\alpha(\omega_N) \end{Bmatrix} \quad \text{and} \quad \mathbf{h}_\beta = \begin{Bmatrix} H_\beta(\omega_1) \\ \vdots \\ \vdots \\ \vdots \\ H_\beta(\omega_N) \end{Bmatrix} \tag{16}$$

$\mathbf{\Phi} = [\mathbf{j}_\alpha\ \mathbf{j}_\beta]$ is a two column matrix where

$$\mathbf{j}_\alpha = \begin{Bmatrix} \varphi_\alpha(x_1)\varphi_\alpha(x_i) \\ \vdots \\ \vdots \\ \vdots \\ \varphi_\alpha(x_N)\varphi_\alpha(x_i) \end{Bmatrix} \quad \text{and} \quad \mathbf{j}_\beta = \begin{Bmatrix} \varphi_\beta(x_1)\varphi_\beta(x_i) \\ \vdots \\ \vdots \\ \vdots \\ \varphi_\beta(x_N)\varphi_\beta(x_i) \end{Bmatrix} \tag{17}$$

The first property given in Section 3.1, Eq. (8) can be used again, demonstrating that the rank of the SFM matrix is less than or equal to 2.

To clarify this point we proceed in the same way as in Section 3.2 to establish the dimension of the subspace generated by the SFM matrix. Let us calculate the product of the SFM matrix by vector

$$\mathbf{v} = \begin{Bmatrix} v_1 \\ : \\ v_i \\ : \\ v_N \end{Bmatrix}$$

which leads to Eq. (18):

$$\mathbf{G}^i\mathbf{v} = \mathbf{\Phi}\mathbf{H}^t\mathbf{v} = \mathbf{\Phi}\begin{bmatrix} a \\ b \end{bmatrix} \tag{18}$$

where the 2 component vector is written as

$$\begin{Bmatrix} a \\ b \end{Bmatrix} = \mathbf{H}^t\mathbf{v} = \begin{Bmatrix} \sum_{j=1}^{N} H_\alpha(\omega_j)v_j \\ \sum_{j=1}^{N} H_\beta(\omega_j)v_j \end{Bmatrix}. \tag{19}$$

In addition, using the particular form of matrix $\mathbf{H}$ (Eq. (16)) in Eq. (18) leads to:

$$\mathbf{G}^i\mathbf{v} = a\mathbf{j}_\alpha + b\mathbf{j}_\beta \tag{20}$$

after straightforward calculation. The subspace generated by the application of matrix $\mathbf{G}^i$ is the linear combination of the 2 vectors $\mathbf{j}_\alpha$ and $\mathbf{j}_\beta$, confirming that in general the matrix rank is equal to 2. However, some particular cases should be underlined, depending on the excitation point and the type of mode responses.

If the excitation is located on a node of a mode, for example mode α, Eq. (17) shows that vector $\mathbf{j}_\alpha = 0$, thus the rank of the SFM matrix is equal to 1 and Eq. (20) is written as:

$$\mathbf{G}^i\mathbf{v} = b\mathbf{j}_\beta, \tag{21}$$

In the same way, if the excitation point is located on a node of both modes α and β it obviously follows that $\mathbf{G}^i\mathbf{v} = 0$ and the rank of the SFM matrix is equal to 0.

Concerning the observation points, it is obvious from Eq. (17) that $\mathbf{j}_\alpha = 0$ if all the measurement points are located on the nodes of mode α, reducing the rank of the SFM matrix to 1 and even to 0 if the measurement points are also nodes of mode β. In general this situation is not observed when the number of observation points is big enough.

Influence of the type of mode is now studied. First Eq. (19) permits establishing Eq. (22):

$$a = \frac{\sum_{j=1}^{N} \dfrac{j\omega_j}{(\Omega_\alpha^2 - \omega_j^2 + 2j\varepsilon_\alpha\Omega_\alpha\omega_j)M_\alpha}v_j}{\sum_{j=1}^{N} \dfrac{j\omega_j}{(\Omega_\beta^2 - \omega_j^2 + 2j\varepsilon_\beta\Omega_\beta\omega_j)M_\beta}v_j}b \tag{22}$$

Initially, two types of modes will be considered: mass and stiffness non resonant modes in the excited frequency band. They are characterized by a frequency response in the excited band of forms:

$$H_\alpha(\omega_j) = \frac{\mathrm{j}\omega_j}{(\Omega_\alpha^2)M_\alpha}, \text{a stiffness type non resonant mode, } \omega_j \ll \Omega_\alpha \tag{23}$$

$$H_\alpha(\omega_j) = \frac{1}{(\mathrm{j}\omega_j)M_\alpha}, \text{a mass type non resonant mode } \omega_j \gg \Omega_\alpha \tag{24}$$

If the two modes are of stiffness non resonant type we can conclude with Eq. (23) that

$$a = \frac{(\Omega_\beta^2)M_\beta}{(\Omega_\alpha^2)M_\alpha}b,$$

whatever the vector $\mathbf{v}$. Consequently, Eq. (20) is written as:

$$\mathbf{G}^i\mathbf{v} = b\left(\frac{(\Omega_\beta^2)M_\beta}{(\Omega_\alpha^2)M_\alpha}\mathbf{j}_\alpha + \mathbf{j}_\beta\right). \tag{25}$$

Even if the 2 modes respond, the total response can be described by a single vector. The rank of the matrix is equal to 1, meaning that the two modes can be grouped in a single contribution.

In the case of two modes of non resonant mass type, the following results can be established:

$$a=\frac{M_\beta}{M_\alpha}b, \mathbf{G}^i\mathbf{v}=b\left(\frac{M_\beta}{M_\alpha}\mathbf{j}_\alpha+\mathbf{j}_\beta\right)$$

and the rank of the SFM matrix is equal to 1 once again.

Lastly, if one mode is of non resonant stiffness type and the second of mass non resonant type, we obtain

$$\left\{\begin{array}{c}a\\b\end{array}\right\}=\left\{\begin{array}{c}\dfrac{1}{(\Omega_\alpha^2)M_\alpha}\displaystyle\sum_{j=1}^{N}\mathrm{j}\omega_j v_j\\ \dfrac{1}{M_\beta}\displaystyle\sum_{j=1}^{N}\dfrac{v_j}{\mathrm{j}\omega_j}\end{array}\right\}.$$

In this case a relation between a and b cannot be established whatever the vector $\mathbf{v}$ and the general form $\mathbf{G}^i\mathbf{v}=a\mathbf{j}_\alpha+b\mathbf{j}_\beta$ applied, indicating that the rank of the SFM matrix is equal to 2.

The case of non resonant modes is interesting when studying the possibility of grouping modes, however their responses are low and they do not contribute significantly to the overall response. The case of resonant modes is of more practical interest. It should first be observed that Eq. (26) holds if two modes have the same natural frequencies and damping:

$$a=\frac{M_\beta}{M_\alpha}b \tag{26}$$

This equation is identical to that of mass type non resonant modes and leads to the same result: both modes can be gathered in one eigenvector. It can be added that the mode shapes have no influence on mode grouping. On the contrary, mode grouping is impossible if the modes have different natural frequencies. In the case of systems with high modal density, an intermediate situation arises because the modes have close natural frequencies and it can be expected that approximate mode grouping will be observed, leading to a reduced dynamic model. In addition, damping is favorable to mode grouping due to the smoothing of the modal frequency response. Strictly speaking, Eq. (26) is in general not satisfied, the rank of the SFM matrix is strictly 2. However, its two non zero eigenvalues will be particular; one of them being much bigger than the second which tends to 0 in the asymptotic case.

3.3.2. *Relation between mode shapes and eigenvectors*

In the following let us consider the case of two modes and an SFM matrix whose rank is equal to 2. By using Eq. (20) for both eigenvectors we obtain:

$$\mathbf{G}^i\mathbf{v}_1=a_1\mathbf{j}_\alpha+b_1\mathbf{j}_\beta=\lambda_1\mathbf{v}_1 \quad \text{and} \quad \mathbf{G}^i\mathbf{v}_2=a_2\mathbf{j}_\alpha+b_2\mathbf{j}_\beta=\lambda_2\mathbf{v}_2 \tag{27}$$

With Eq. (27) the following can be derived:

$$\mathbf{j}_\alpha=c_\alpha\mathbf{v}_1+d_\alpha\mathbf{v}_2 \quad \text{and} \quad \mathbf{j}_\beta=c_\beta\mathbf{v}_1+d_\beta\mathbf{v}_2 \tag{28}$$

It is now straightforward to demonstrate that the eigenvectors can be used as an equivalent basis for the 2 mode shapes. Whatever the excitation of the two modes, it is possible to write the vector of the velocity response with the two mode shapes.

$$\{W(x_j,t)\}=A_\alpha(t)\{\varphi_\alpha(x_j)\}+A_\beta(t)\{\varphi_\beta(x_j)\}, \tag{29}$$

In order to introduce vectors $\mathbf{j}_\alpha$ and $\mathbf{j}_\beta$ as defined in Eq. (17), Eq. (29) is modified:

$$\{W(x_j,t)\}=\frac{A_\alpha(t)}{\varphi_\alpha(x_i)}\mathbf{j}_\alpha+\frac{A_\beta(t)}{\varphi_\beta(x_i)}\mathbf{j}_\beta$$

Finally, by taking Eq. (28) into account, we obtain:

$$\{W(x_j,t)\}=\left(\frac{A_\alpha(t)}{\varphi_\alpha(x_i)}c_\alpha+\frac{A_\beta(t)}{\varphi_\beta(x_i)}c_\beta\right)\mathbf{v}_1+\left(\frac{A_\alpha(t)}{\varphi_\alpha(x_i)}d_\alpha+\frac{A_\beta(t)}{\varphi_\beta(x_i)}d_\beta\right)\mathbf{v}_2 \tag{30}$$

This expression demonstrates the possibility of using the eigenvectors of the SFM matrix to express the velocity response to all types of excitation. It is important to note here that even if the eigenvectors are associated with a particular point of excitation they can be used for any excitation point and even for distributed loads. Of course, if an excitation point used for

building the SFM matrix is located on a node of a mode, it is eliminated from the modal basis and will lead to errors when eigenvectors are used to express responses in a general case of excitation.

3.4. General case

The results obtained in the previous sections when 1 or 2 modes were responding can be generalized as follows.

Let us introduce the eigenvalues λ_α^i and eigenvectors $\mathbf{v}_\alpha^i$ of the SFM matrix, where α is the order of the eigenvalue such that:

$|\lambda_1^i| \geq |\lambda_2^i| \geq \ldots \geq |\lambda_P^i|$ and P is the rank of the SFM matrix

The velocity vector of the system can be written as:

$$\mathbf{w}(t) = \sum_{\alpha=1}^{P} a_\alpha^i(t)\mathbf{v}_\alpha^i \tag{31}$$

with

$$\{a_\alpha^i(t)\} = [\langle \mathbf{v}_\alpha^i . \mathbf{v}_\beta^i \rangle]^{-1}\{\langle \mathbf{v}_\beta^i \boldsymbol{w}(t) \rangle\} \tag{32}$$

where $[]^{-1}$ indicates the inverse matrix and $\langle\ \rangle$ the scalar product of two vectors.

Basically, the rank of the SFM matrix is equal to the number of modes that effectively participate in the vibration field. As shown in Section 3.2, the more a mode responds the higher the associated eigenvalue, thus taking into account contributions of larger eigen values permits taking into account modes with high participation factors. However contributions of modes having frequency responses with the same variation in the excited band can be grouped in one eigenvector, thereby reducing the rank of the matrix. This is the case of non resonant contributions of the same type (mass or stiffness) and resonant modes with the same natural frequency and damping. When proportionality is verified approximately, the contributions of modes are not fully grouped in the same non zero eigenvalue, but in one very large eigenvalue and other small eigenvalues of the SFM matrix. This property is of major interest for high modal density systems where numerous modes contribute to the vibration field and have similar frequency responses (in particular when modal overlap is achieved) and can thus be grouped in one eigenvector.

It can be concluded that to describe the vibration behavior of a system of high modal density, the contributions of small eigenvalues can be neglected, limiting the summation in Eq. (31) to the terms with large eigenvalues.

If the eigenvectors are calculated from the SFM matrix obtained with a particular point of excitation that conserves all the dominant modes, then they can be used for calculating responses to all types of excitation.

4. Application to longitudinal beam vibrations

4.1. Calculation of the SFM matrix

In this section, the approach is applied to longitudinal beam vibrations. This simple case was chosen to test the approach, because exact solutions are available.

A beam of length L, cross section S, and made of homogeneous material, is excited longitudinally by a harmonic force of unit amplitude at point x_i. The response at point x_j can be easily calculated (see Guyader [30], chapter 10) with the result written as:

$$W^i(x_j,t) = c\frac{\sin\Big(k(1-\mathrm{j}\eta)(L-x_j)\Big)\sin(k(1-\mathrm{j}\eta)x_i)}{(1+\mathrm{j}\eta)\sin(k(1-\mathrm{j}\eta)L)}\exp(\mathrm{j}\omega t) \quad \text{if } x_i < x_j \tag{33a}$$

$$W^i(x_j,t) = c\frac{\sin(k(1-\mathrm{j}\eta)(L-x_i))\sin(k(1-\mathrm{j}\eta)x_j)}{(1+\mathrm{j}\eta)\sin(k(1-\mathrm{j}\eta)L)}\exp(\mathrm{j}\omega t) \quad \text{if } x_i > x_j \tag{33b}$$

Here c is the wave speed, $k = \omega/c$ is the wave number and η is the damping loss factor of the material. The non dimensional angular frequency used in the following is defined as:

$$\nu = \frac{\omega L}{c\pi}$$

The two expressions (33) permitted the calculation of the SFM matrix and then the determination of its eigenvalues and eigenvectors. 150 equally spaced points of calculation and 150 frequencies in the excited band were considered in all the examples presented.

One important parameter is the modal overlap factor Δ, defined as:

$$\Delta = \eta \frac{n\omega}{2\pi}$$

where η is the damping loss factor, n the modal density and ω the angular frequency.

In the case of the longitudinal vibration of a beam, using the asymptotic modal density $n = 2L/c$ and the non dimensional frequency v, the modal overlap factor is written simply as:

$$\Delta = \eta v$$

In the first case, a beam driven at point 0.366 L is considered. It is excited in the non dimensional frequency band [9.5, 27.5], that is to say the resonance frequencies of modes 10–27 are in the excited band. In the first case the damping loss factor is equal to 0.005 and the modal overlap factor is small (varying from 0.0475 to 0.1375 in the excited band).

Fig. 1 presents the frequency response at point 0.033 L; it is dominated by 18 well-separated modes.

4.2. Eigenvalues of the SFM matrix

In Fig. 2, the 30 lowest modules of the SFM matrix eigenvalues are plotted. It is clear that 18 eigenvalues are significant, corresponding to the number of resonant modes in the excited band.

When modal overlap is increased by way of a larger damping loss factor (η=0.06), and by keeping all the other parameters the same as in the previous case, the frequency response is smoothed as shown in Fig. 3, making it impossible to perform the mode count.

The moduli of the SFM matrix eigenvalues are shown in Fig. 4. It can be seen that they are smaller compared to the previous case of low damping and less than 18 eigenvalues contribute significantly, which can be explained by mode grouping. However, increasing damping also reduces the effectiveness of the high order modes and the two effects lead to the result presented.

4.3. Eigenvectors of the SFM matrix, effective shapes

The eigenvectors of the SFM matrix are used as the basis for building dynamic models with the approach developed in the previous section. Thus it is important to describe their behavior. The case of a beam in longitudinal motion excited at point 0.366 L is considered. It is excited in the non dimensional frequency band [9.5, 27.5], that is to say modes 10–27 have their resonance frequencies in the excited band. In the first case the damping loss factor is equal to 0.005 and the modal overlap factor varies from 0.0475 to 0.1375 in the excited band.

In the following, eigenvectors are presented by plotting a continuous effective shape function obtained from the values of the eigenvector components in 150 points spaced equally along the beam. Fig. 5 shows the plots of the imaginary and real parts of the first, second and eleventh effective shapes. The decomposition of beam displacements with Eq. (31) indicates that shape functions represent displacements along the beam that can be used as an elementary motion to decompose the velocity field. Shape functions oscillate around zero with an average wavelength that varies slightly with the eigenvalue order. The average wavelength of the first effective shape is approximately equal to 2 L/22, while those of the

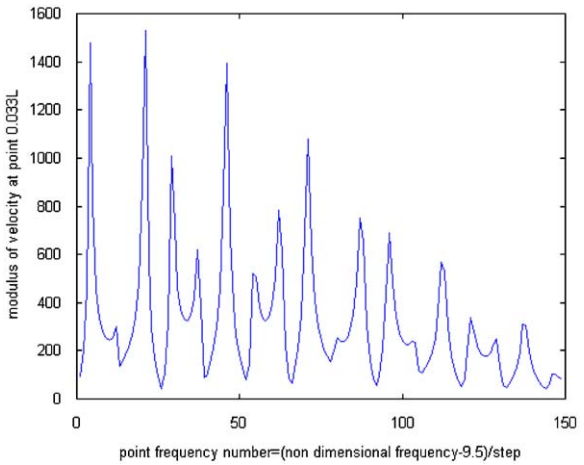

Fig. 1. Frequency response modulus at point 0.033 L, for a lightly damped beam excited at point 0.366 L. Excitation in the non dimensional frequency band [9.5, 27.5], modes of order 10–27 are resonant in the band. Damping loss factor equal to 0.005, modal overlap factor varying from 0.0475 to 0.1375 in the band.

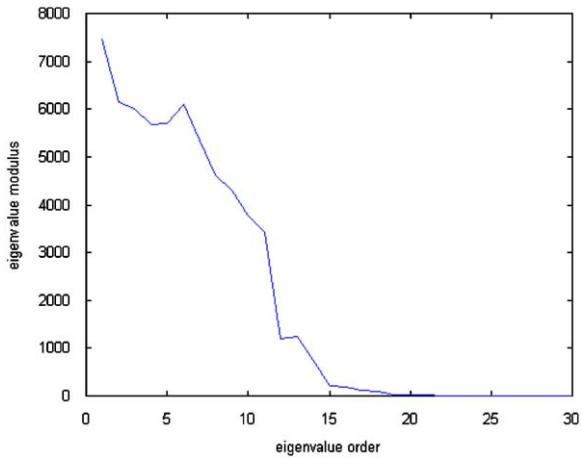

Fig. 2. Modulus of SFM matrix eigenvalues of a lightly damped beam excited at point 0.366 L. Excitation in the non dimensional frequency band [9.5, 27.5], modes of order 10–27 are resonant in the band. Damping loss factor equal to 0.005, modal overlap factor varying from 0.0475 to 0.1375 in the band.

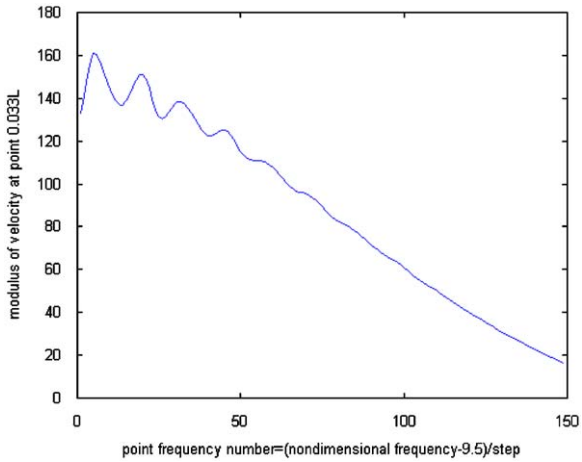

Fig. 3. Frequency response modulus at point 0.033 L for a highly damped beam excited at point 0.366 L. Excitation in the non dimensional frequency band [9.5, 27.5], modes of order 10–27 are resonant in the band. Damping loss factor equal to 0.06, modal overlap factor varying from 0.57 to 1.65 in the band.

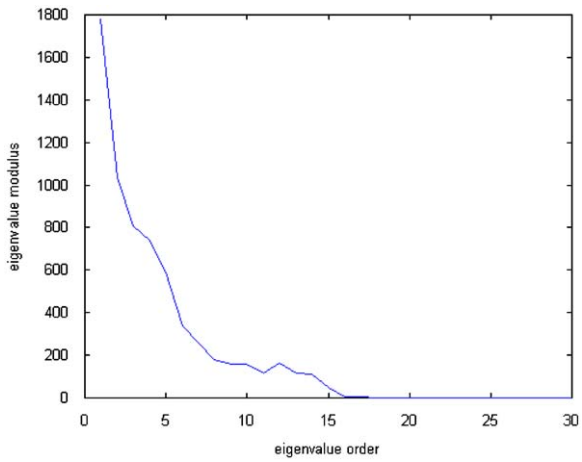

Fig. 4. Modulus of SFR matrix eigenvalues, with the highly damped beam excited at point 0.366 L. Excitation in the non dimensional frequency band [9.5, 27.5], modes of order 10–27 are resonant in the band. Damping loss factor equal to 0.06, modal overlap factor varying from 0.57 to 1.65 in the band.

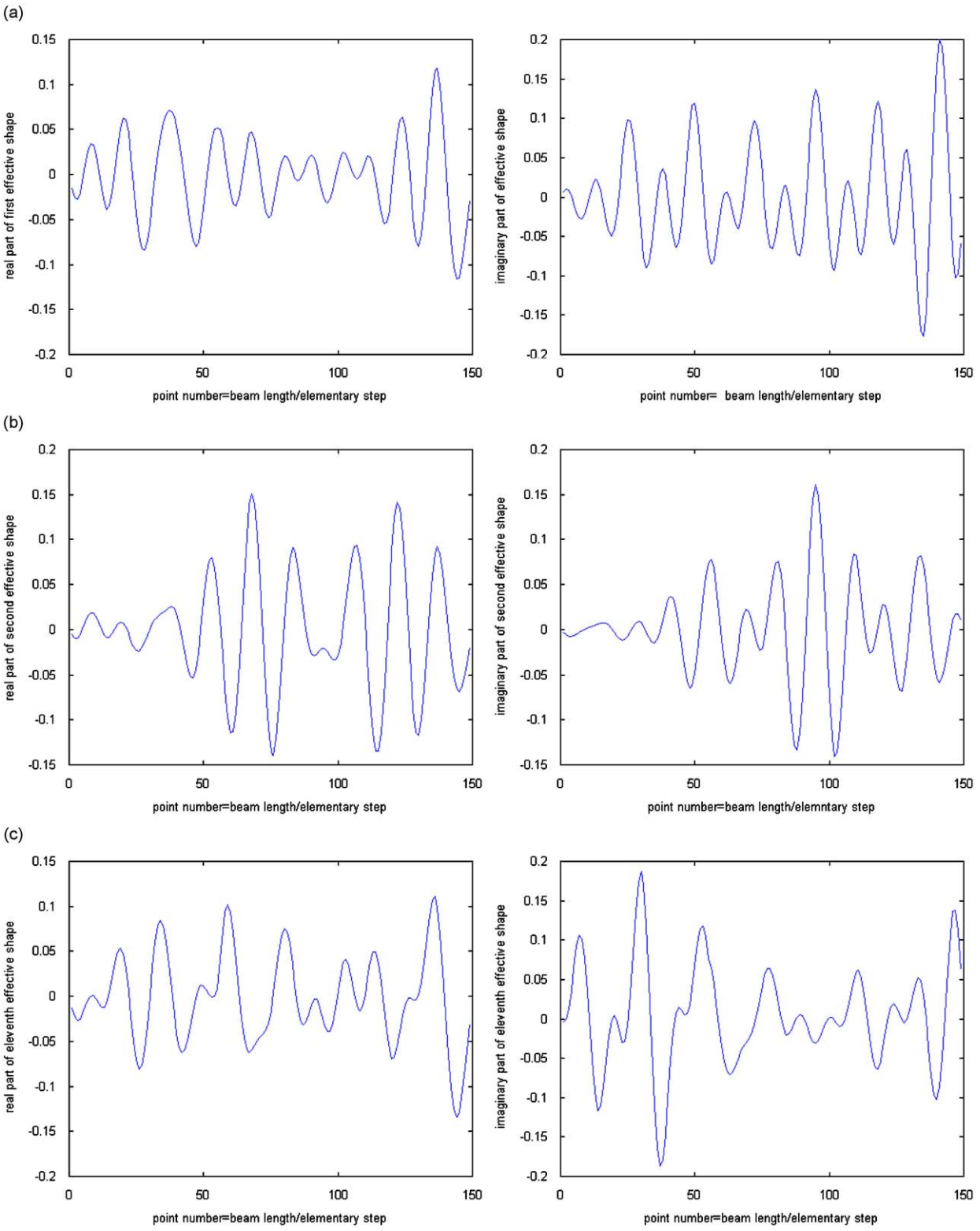

Fig. 5. Real and imaginary parts of different effective shapes for lightly damped beam. Excitation point 0.366 L, damping loss factor 0.005, modal overlap varying from 0.0475 to 0.1375. Non dimensional frequency band [9.5, 27.5], modes 10–27 are resonant. (a) First eigenvector, (b) second eigenvector, and (c) eleventh eigenvector.

second and eleventh effective shapes are similar. All these values lay between the maximum and minimum mode wave lengths in the excited band which vary here from 2 L/10 to 2 L/27. In addition the imaginary part has an obvious similarity with the real part.

When the excitation point is modified, the effective shapes are obviously also modified.

Damping has an influence on effective shapes, and by comparing Fig. 6 (high damping) and Fig. 5 (low damping) it can be seen that the average wavelength of the effective shapes increases with damping. This is due to the fact that damping has influenced the high frequencies more than the low frequencies. However, the wavelength of the effective shapes still remains between the maximum and minimum wavenumbers of the resonant modes. A second phenomenon associated with high modal overlap is the localization of the high amplitude of the effective shapes at the location of the excited point.

4.4. Building dynamic models

The aim of this section is to use a simple case to illustrate how the eigenvectors of the SFM matrix (effective shapes) can be used to decompose vibration fields and how approximation can be obtained by reducing the number of effective shapes taken into account in the calculation.

When decomposed on the eigenvectors of the SFM matrix, the vibration field takes the form given in Eq. (31). Decreasing the number M of eigenvectors used leads to an increasingly approximated vibration field. Good approximation can be expected when the eigenvectors associated with the dominant eigenvalues are taken into account. To clarify this

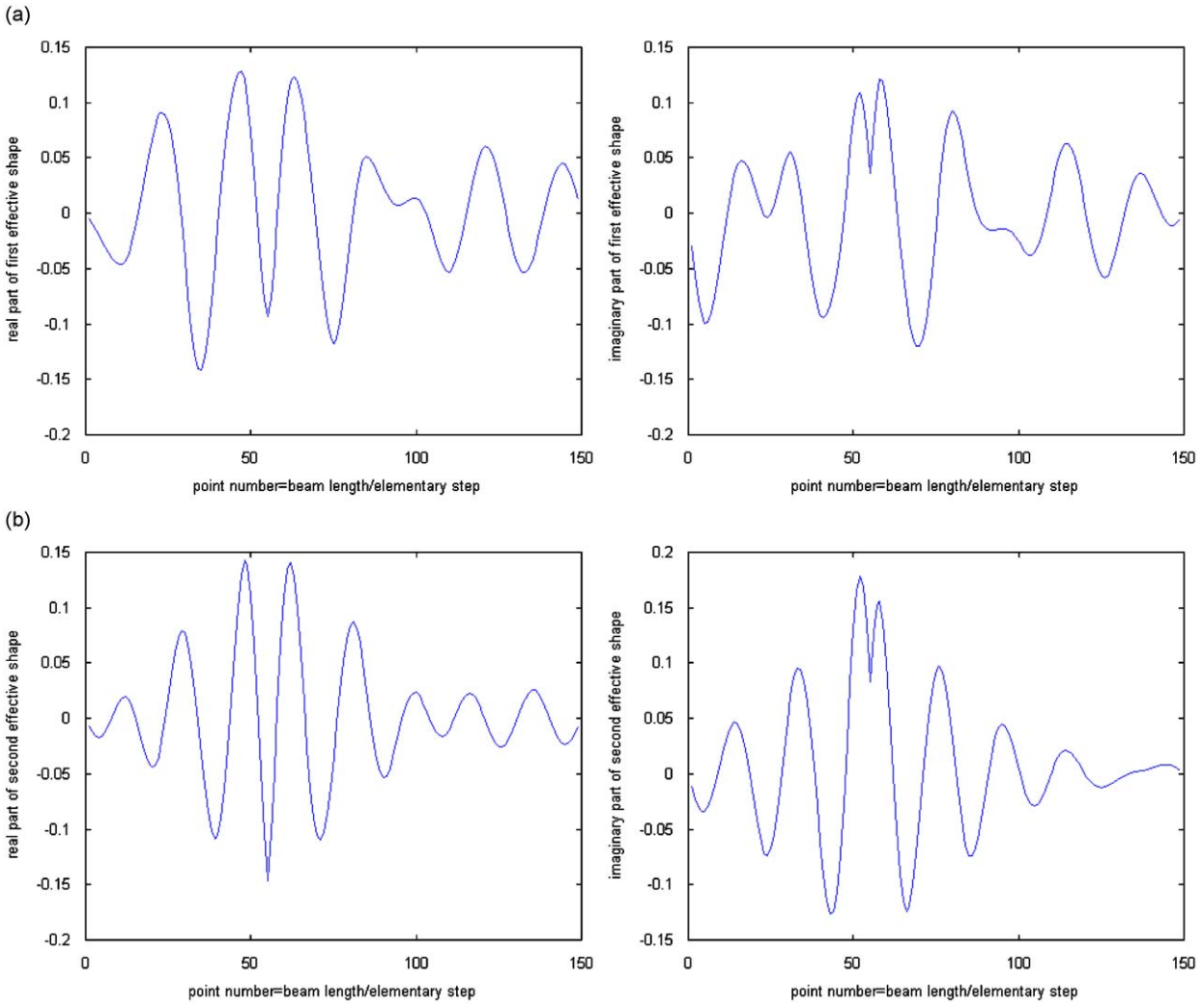

Fig. 6. Real and imaginary part of different effective shapes for lightly damped beam. Excitation at point 0.366 L, damping loss factor 0.06, modal overlap varying from 1.14 to 3. Non dimensional frequency band [9.5, 27.5], modes 10–27 are resonant. (a) First eigenvector, and (b) second eigenvector.

point, the example of a beam in longitudinal motion is used again, with the SFM matrix built as in Section 4.1. To calculate the beam response at instant t the excitation vector must be defined as $\mathbf{F}^i(t) = \{A_k^i \exp(j\omega_k t)\}$. Obviously, each given force type leads to a specific excitation vector; however, the entire force time history can be built by summation of the impulses at different instants. Consequently the results obtained from an impulse force indicate the general behavior. For the sake of simplicity, we consider in the following the case of an impulse force applied at instant t=0. After application of the Fourier transform, the force vector is written as $\mathbf{F}^i(t) = \{\exp(j\omega_k t)\}$. In this excitation vector, all the frequency components have the same amplitude, but the finite size of the vector indicates that the impulse excitation is filtered in the angular frequency band $[\omega_1, \omega_N]$. Due to the increment $\delta\omega$ in the angular frequency characterizing two consecutive components of the force vector, the time history can be built up to a maximum time $T_{\max} = 2\pi/\delta\omega$.

First the case of Fig. 2 is considered. A beam is excited at point 0.366 L in a non dimensional frequency band [9.5, 27.5] such that the modes of order 10–27 are resonant (150 equally spaced angular frequencies are considered in the excited band). The damping loss factor is equal to 0.005 and the modal overlap factor is small (varying from 0.0475 to 0.1375 in the excited band). The SFM matrix is calculated using the same excitation point.

In Fig. 7, the beam response at instant t=0.098 ($T_{\max}$=0.4902) is reconstructed for variable numbers of eigenvectors. When 18 eigenvectors are used, that is to say the number of resonant modes, the comparison with the exact response

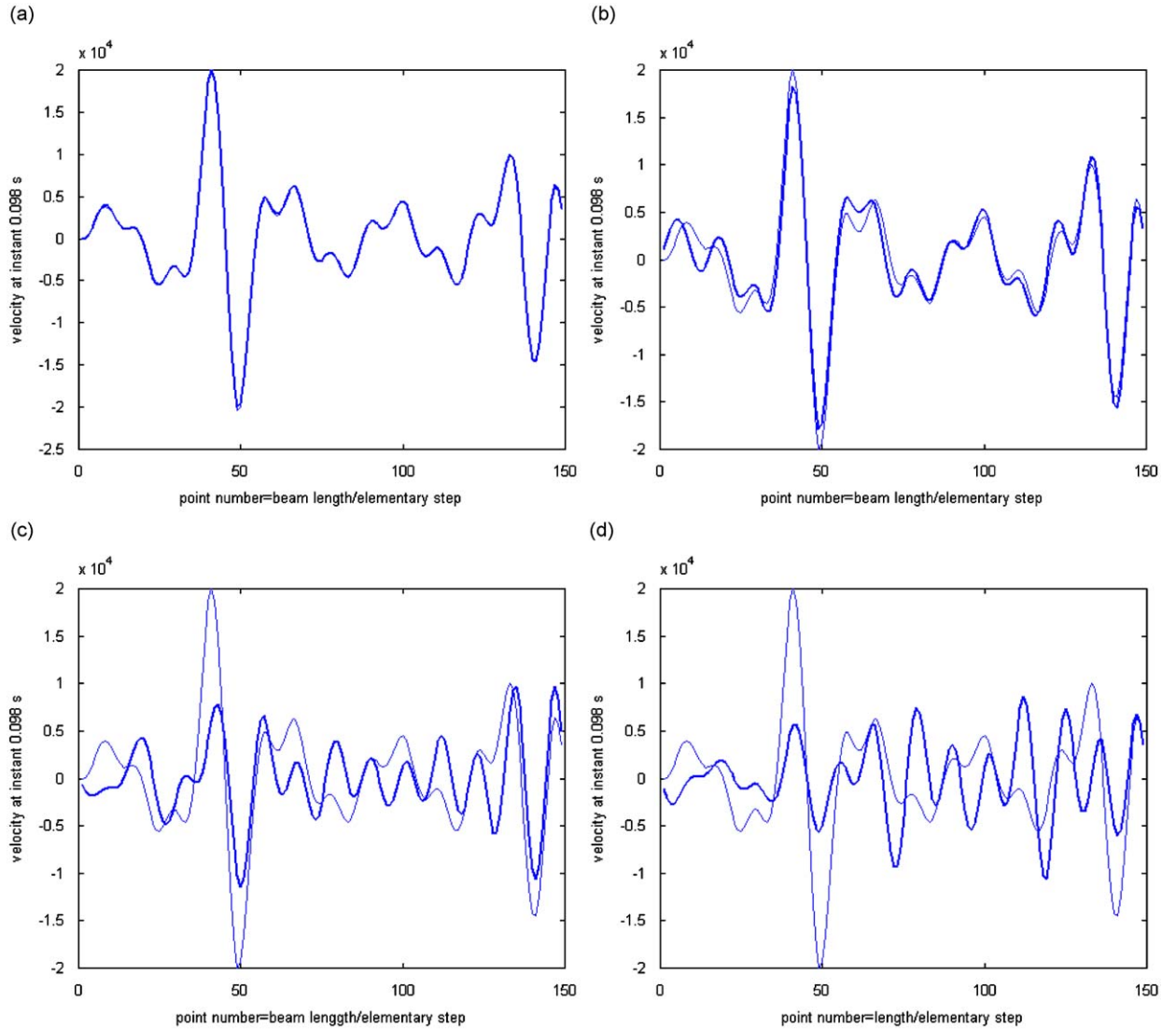

Fig. 7. Comparison of exact and reconstructed (thick line) displacements along the beam at instant t=0.098, for different number of SFM matrix eigenvectors. Beam excited at point 0.366 L, in the non dimensional frequency band [9.5, 27.5] such that modes of order 10–27 are resonant. Damping loss factor equal to 0.005. Modal overlap factor varying from 0.0475 to 0.1375, in the excited band. (a) 18 eigen vectors, (b) 10 eigen vectors, (c) 6 eigen vectors, and (d) 3 eigen vectors.

obtained by using the complete SFM matrix is almost exact. When a reduced number of eigenvectors is used (10, 6 and 3), the predicted beam response is increasingly approximated, demonstrating that significant information is ignored.

The same case is studied (Fig. 8), but here the eigenvectors are those of the SFM matrix calculated for excitation point 0.0333 L which is different from that used for calculating the beam response (0.366 L). The excitation point used for calculating the eigenvectors is chosen close to the extremity so that it does not correspond to a node of a resonant mode.

When 18 eigenvectors are considered, the prediction agrees very well with the exact result, demonstrating that the eigenvector basis can be built by using any excitation point but not by a node of modes dominating the beam response. When 10 eigenvectors are considered, the prediction is not as good as it was in Fig. 7, due to the fact that the eigenvectors of the SFM matrix include the information on the excitation point used to establish it. Thus they fit perfectly with the beam response description when the beam is excited at the same point used for building the SFM matrix.

In the second example the same case with an increased damping loss factor (η=0.06) is used, with a modal overlap factor varying from 0.57 to 1.65 in the band. The corresponding eigenvalues were given in Fig. 4, while the reconstruction results are presented in Fig. 9. Using 10 eigenvectors to reconstruct the displacement field permits quite precise prediction

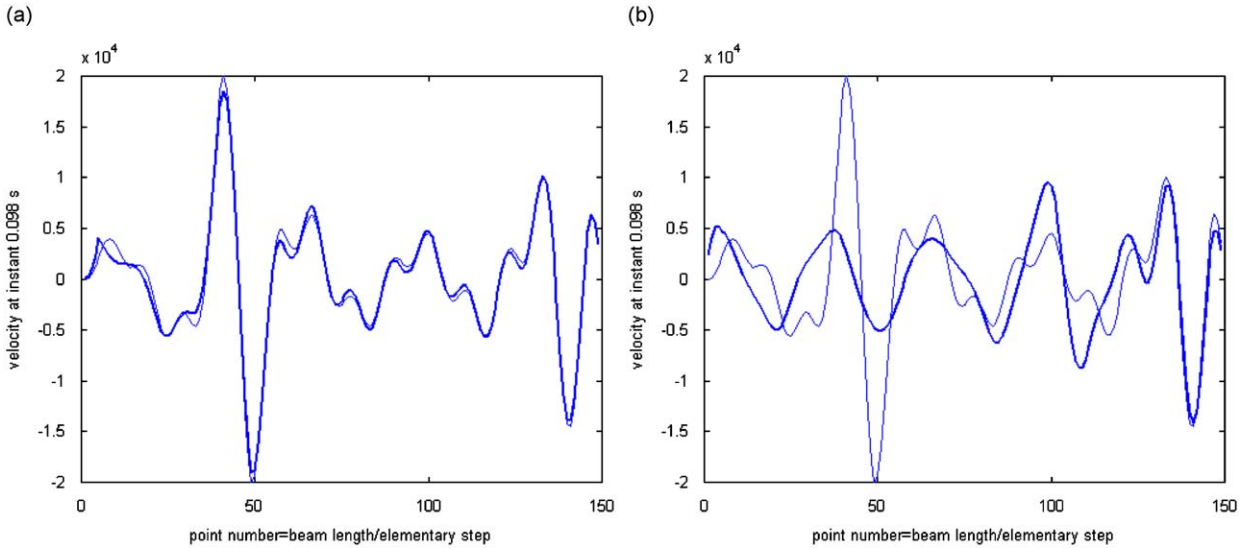

Fig. 8. Comparison of exact and reconstructed (thick line) displacements along the beam at instant t=0.098, for different number of SFM matrix eigenvectors corresponding to excitation at point 0.0333 L. Beam excited at point 0.366 L, in the non dimensional frequency band [9.5, 27.5] such that modes of order 10–27 are resonant. Damping loss factor equal to 0.005. Modal overlap factor varying from 0.0475 to 0.1375 in the excited band. (a) 18 eigen vectors, and (b) 10 eigen vectors.

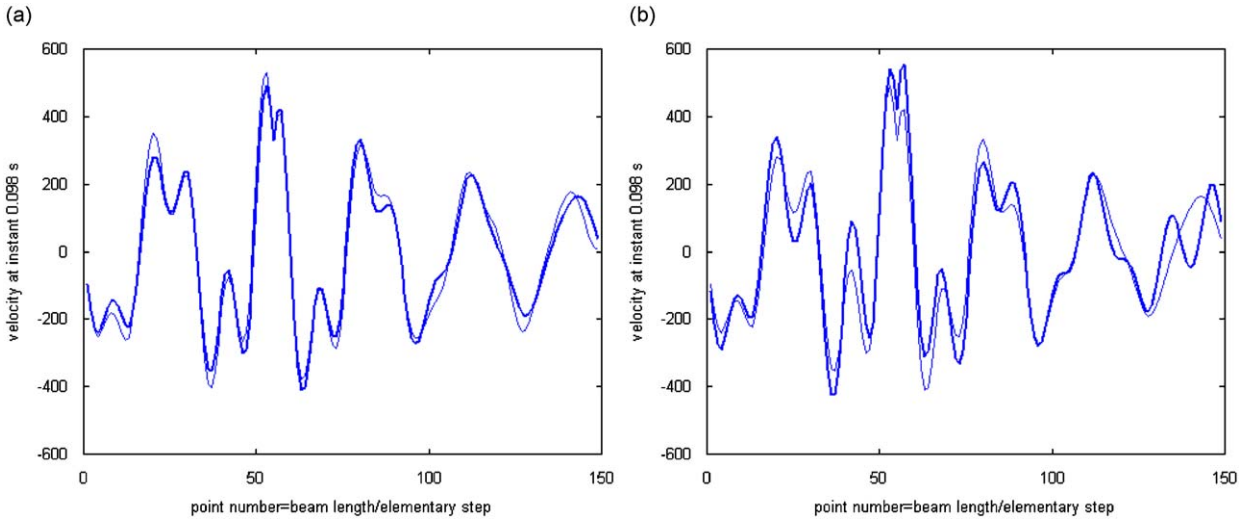

Fig. 9. Comparison of exact and reconstructed (thick line) displacements along the beam at instant t=0.098, for different number of SFM matrix eigenvectors. Beam excited at point 0.366 L, in the non dimensional frequency band [9.5, 27.5] such that modes of order 10–27 are resonant. Damping loss factor equal to 0.06. Modal overlap factor varying from 0.57 to 1.65 in the excited band. (a) 10 eigen vector, and (b) 3 eigen vectors.

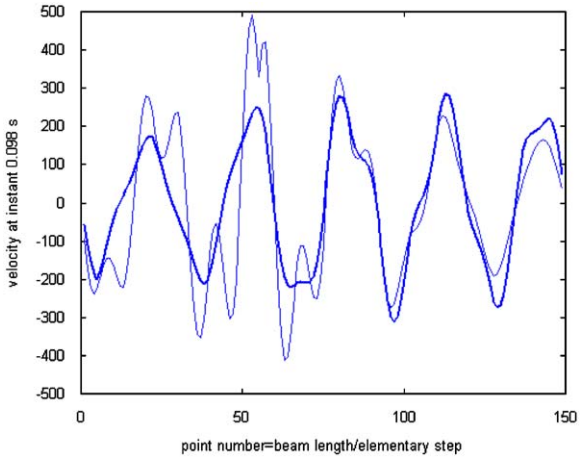

Fig. 10. Comparison of exact (thin line) and reconstructed (thick line) displacements along the beam at instant t=0.098, for 10 SFM matrix eigenvectors corresponding to excitation at point 0.0333 L. Beam excited at point 0.366 L, in the non dimensional frequency band [9.5, 27.5] such that modes of order 10–27 are resonant. Damping loss factor equal to 0.06. Modal overlap factor varying from 0.57 to 1.65 in the excited band.

and good approximation is achieved with only 3 eigenvectors. This provides a good illustration of mode grouping achieved by smoothing the frequency modal responses with high damping. When the excitation point used to build the SFM matrix is different from the beam excitation point, the response calculated with a reduced model of 9 eigenvectors continues to describe vibration behavior (see Fig. 10), but agreement is not so good as it was in Fig. 9.

4.5. Energy prediction with reduced model

In certain vibroacoustic problems, the energy of vibrating systems is of greater interest than the displacement fields, as the advantage of global prediction associated with energy is that the results are more robust. The energy time history of vibrating systems can be calculated with the present approach and it can be assumed that a strongly reduced model is sufficient to obtain a reasonable prediction. To investigate this point we consider the case of Fig. 9. The energy descriptor considered in the following is the quadratic velocity of the excited structure defined by:

$$E(t) = \sum_{j=1}^{N} (W(x_j, t))^2 = \langle \mathbf{W}(t)\mathbf{W}(t) \rangle \tag{34}$$

where $\langle \mathbf{W}(t)\mathbf{W}(t) \rangle$ indicates the scalar product of the vectors.

In Fig. 11, the level of error (L_E) between the exact and approximated quadratic displacements is plotted versus the number of degrees of freedom of the reduced model.

$$L_E = 10\,\mathrm{Log}(E_{\mathrm{app}}(t)/E_{\mathrm{exact}}(t))$$

A prediction of beam quadratic velocity at a given instant can be approximated with a reduced model of small size. If an approximation of 3 dB is sufficient, which is what is accepted in practice, then three (resp. six) dof are necessary in case of high (resp. low) modal overlap.

Fig. 12 shows the energy response calculated when the SFM matrix is built with an excitation point different from that used for calculating the beam response. Model reduction is not as efficient as it was previously but remains true particularly for a high modal overlap factor. For example, if a 3 dB approximation is sufficient, models with 13 dof (η=0.005) and 5 dof (η=0.06) are necessary. As expected, these models are slightly bigger than previously when the SFM matrix was obtained with the same excitation point as the beam response.

5. The case of rectangular SFM matrices

Under experimental conditions the measured SFM Matrix can be rectangular. For example, the number of space points can be lower than the number of frequency points. The SVD technique is often used when rectangular matrices are considered, however to obtain the physical meaning of effective shapes in the same way as before, the approach described above can be extended by including lines of 0 in the rectangular matrix to obtain a square one, called squared SFM matrix in the following. Obviously, the rank of the squared SFM matrix is identical to that of the rectangular matrix, meaning that the basic property described in Section 3 remains true. In addition, no physical information is lost in the squared SFM matrix because the modes controlling the frequency response remain unchanged.

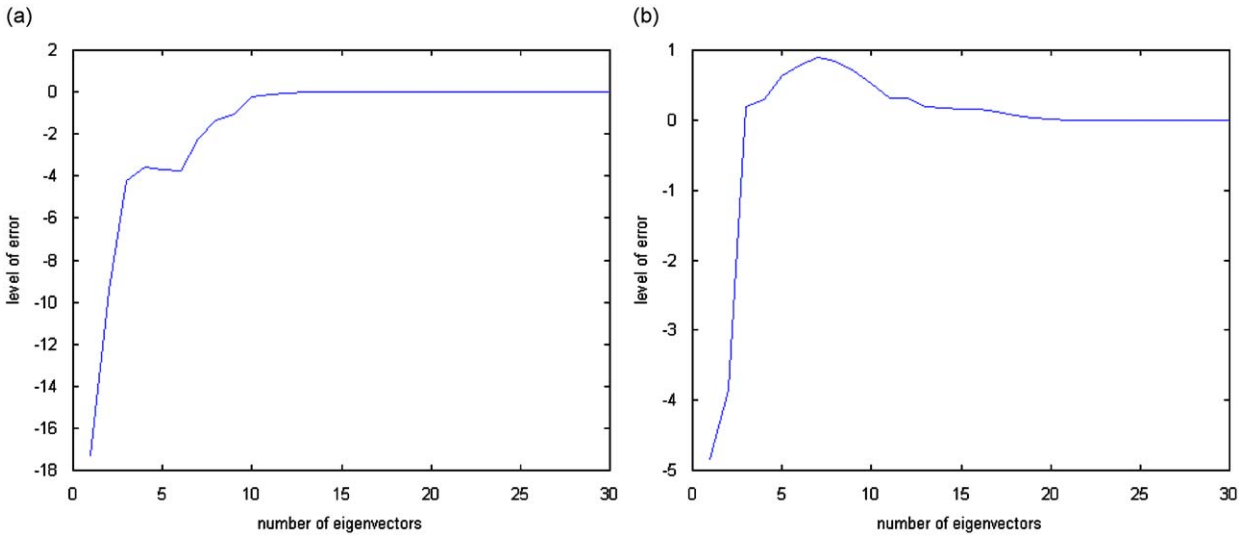

Fig. 11. Level of error between exact and approximated quadratic displacements at instant t=0.098 versus the number of SFM matrix eigenvectors. Beam excited at point 0.366 L, in the non dimensional frequency band [9.5, 27.5] such that modes of order 10–27 are resonant. Damping loss factor equal to: (a) 0.005, and (b) 0.06.

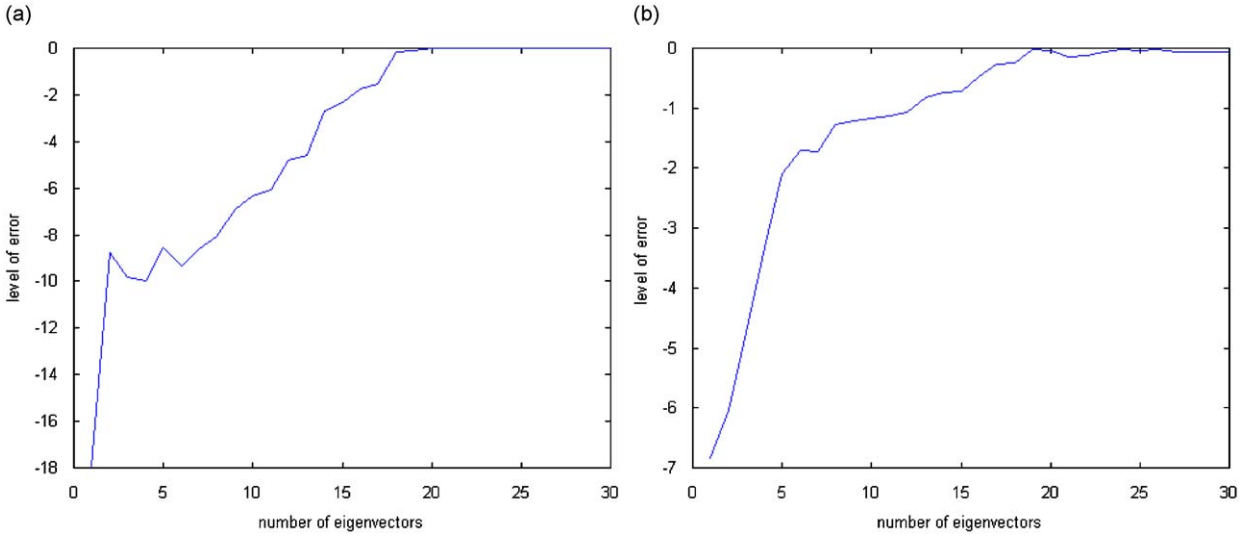

Fig. 12. Level of error between exact and approximated quadratic displacements at instant t=0.098 versus the number of SFM matrix eigenvectors corresponding to excitation at point 0.0333 L. Beam excited at point 0.366 L, in the non dimensional frequency band [9.5, 27.5] such that modes of order 10–27 are resonant. Damping loss factor equal to: (a) 0.005, and (b) 0.06.

As mentioned in Section 3.2, the eigenvalues depend on the number of space points, thus the eigenvalues of the squared SFM matrix cannot be expected to be identical to those of the square SFM matrix obtained with a higher number of space points. Thus the results obtained by squared SFM and classical SFM matrices have to be compared by using reconstructed vibrations rather than at the intermediate stage of the eigenvalues and eigenvectors. A numerical example was studied describing the behavior of a beam excited at point 0.366 L in a frequency band where 18 resonant modes were excited. This example corresponds to the case of the highly damped beam shown in Fig. 9. A squared SFM matrix built from a rectangular SFM matrix with 150 frequency points and 80 space points was considered. The responses are plotted in Fig. 13 and compared to those of a classical SFM matrix whose number of space points was increased to 150.

The response obtained with the squared SFM matrix has nil components at the point located outside the beam, corresponding to the number of 0 lines added. The non zero components calculated with 10 eigenvectors agree reasonably with the exact beam response in which 18 resonant modes contribute. However, the results of Fig. 9 calculated from a

classical SFM matrix with 150 space points not only have better spatial definition, but also better agreement between approximated and exact responses.

In conclusion, the use of the present approach to the rectangular SFM matrix is straightforward, but the approximation obtained with a reduced number of eigenvectors is slightly poorer in comparison to that of the square SFM matrix. To obtain the same precision when using a rectangular SFM matrix instead of a square SFM matrix, more eigenvectors have to be considered. As a rule of thumb based on the result obtained in the beam example, an increase of 10% seems reasonable.

6. Experimental validation

In order to verify whether the approach can be used experimentally, we measured the SFM matrix on a clamped aluminum plate of thickness 0.003 m, length 1.5 m and width 0.95 m. The driving force was generated by a shaker placed at point (0.93, 0.35), and the velocity was measured by a laser vibrometer at 851 positions placed on a grid of 23 by 37 locations. The modal density of the plate was equal to 0.1732 modes/Hz. The frequency band under study varied from 700 to 1550 Hz and measurements were performed with one hertz resolution. The band contained 147 resonant modes.

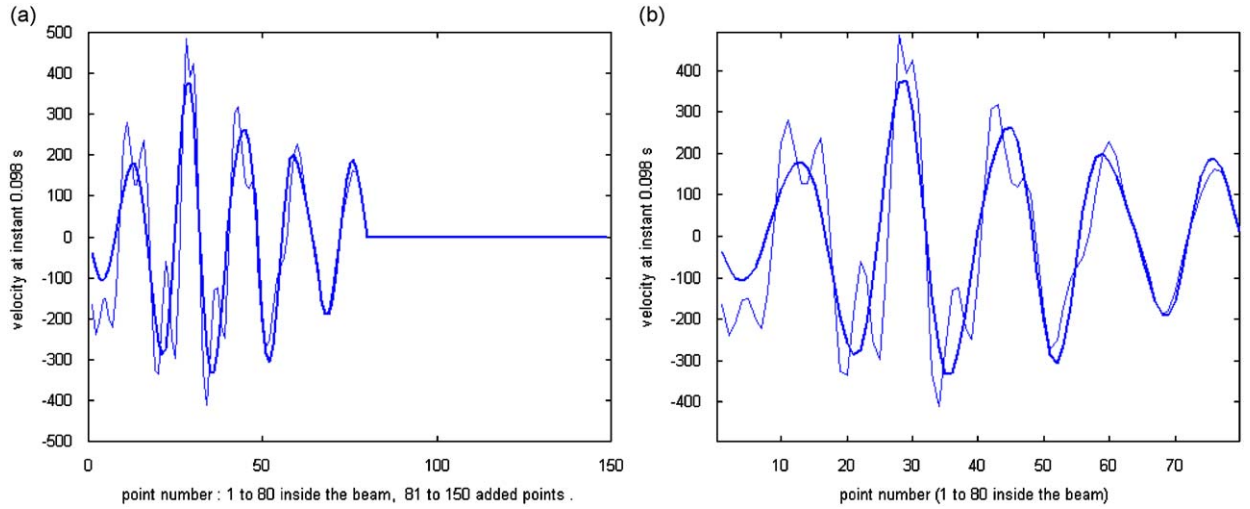

Fig. 13. Comparison of exact (thin line) and reconstructed (thick line) velocities at instant t=0.098, for 10 SFM matrix eigenvectors obtained with a rectangular matrix (80×150). Beam excited at point 0.366 L, in the non dimensional frequency band [9.5, 27.5] such that modes of order 10–27 are resonant. Damping loss factor equal to 0.06. Modal overlap factor varying from 0.57 to 1.65 in the excited band. Rectangular SFM matrix of 80 space points and 150 frequency points. (a) Physical and added points, and (b) physical points inside the beam.

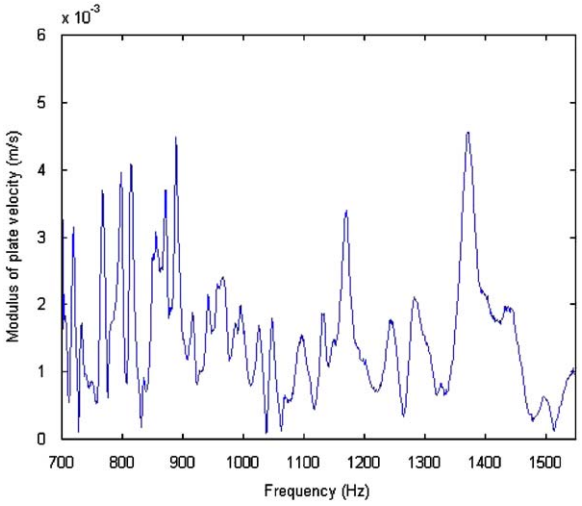

Fig. 14. Velocity modulus at point (0.042, 0.52) versus the frequency, case of a rectangular clamped aluminum plate excited at point (0.93, 0.35) by a unit force. Plate dimensions are: thickness 0.003, width 0.94, and length 1.5.

An example of the frequency response function is presented in Fig. 14. It was measured at point (0.042, 0.52) located near the edge of the plate and numerous modes can be seen to participate in the response. Also, modal overlap is achieved for high frequencies in the band but not for low frequencies.

The SFM matrix was built from measured velocities and then calculated eigenvalues of which the first 300 are plotted in Fig. 15. It can be seen that the high order eigenvalues do not reach zero in comparison to the theoretical cases studied in Section 3. This is due to measurement uncertainties.

The plate velocity field at observation time t=0.0667, resulting from impulse excitation at t=0, is presented in Fig. 16 for different sizes of the reduced model. When 75 eigenvectors are considered, the vibration field is almost identical

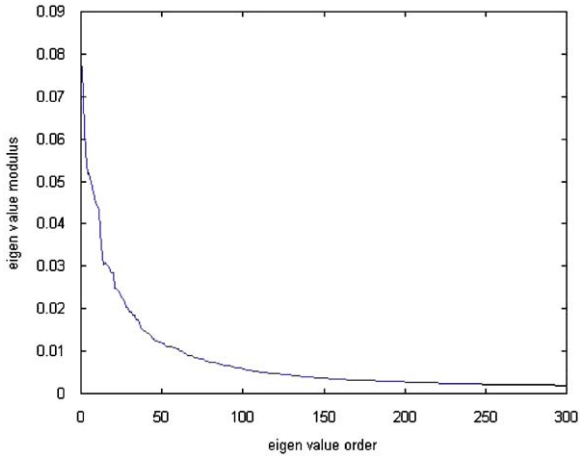

Fig. 15. Eigenvalues of SFM matrix of a rectangular clamped aluminum plate excited at point (0.93, 0.35) by a unit force in the frequency band from 700 Hz to 1551 Hz. Plate dimensions are: thickness 0.003, width 0.94, length 1.5.

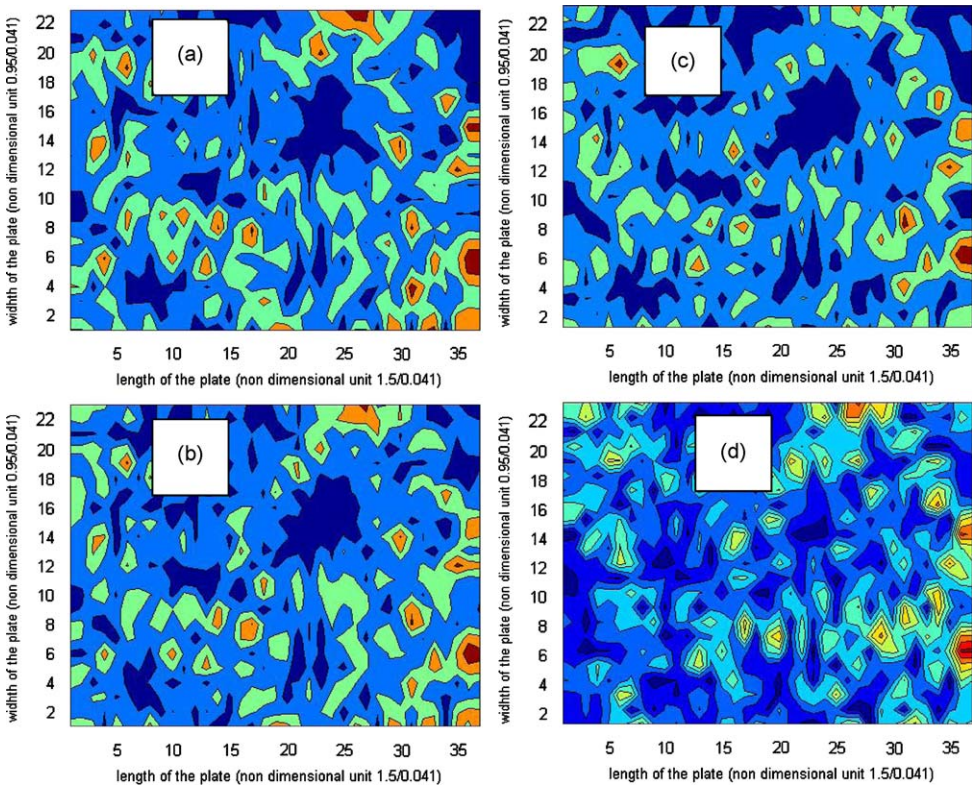

Fig. 16. Velocity field at instant t=0.0667 of a rectangular clamped aluminium plate excited at point (0.93, 0.35) by a unit impulse force filtered in the frequency band from 700 to 1551 Hz. Plate dimensions are: thickness 0.003, width 0.94, length 1.5. (a) Exact result, reduced model with (b) 75 dof, (c) 50 dof, and (d) 25 dof.

to the exact one and the result remains quite good when 50 eigenvectors are used. Differences appear for 25 eigenvectors even if the global tendency is captured. Surprisingly, very large vibrations appear at some boundary points of the contour map. However, the boundary points of the map do not correspond to the clamped boundary points of the plate, being located 4 cm from it. As mentioned previously, 147 resonant modes contribute to the response and the plate velocity field is almost exact when 75 effective shapes are used to calculate the response. As expected, decreasing the size of the reduced model leads to an approximation of the response that nonetheless remains acceptable up to 25 effective shapes.

Lastly, the level of energy error $L_{er}(t)$ versus the number of dof of the reduced model is presented in Fig. 17.

$$L_{er}(t) = 10\,\mathrm{Log}\left(\frac{\int_s (V_{\mathrm{app}}(M,t))^2\,\mathrm{d}m}{\int_s \left(V_{\mathrm{exact}}(M,t)\right)^2\,\mathrm{d}m}\right)$$

where $\int_s (V_{\mathrm{app}}(M,t))^2\,\mathrm{d}m$, is the approximated quadratic velocity and $\int_s (V_{\mathrm{exact}}(M,t))^2\,\mathrm{d}m$, the exact one.

Due to the frequency band of the calculation (up to 1551 Hz) and the frequency step of 1 Hz, the possible observation time must be located in the interval from 0.00064 to 1 s. The global tendency of the approximation versus the size of the

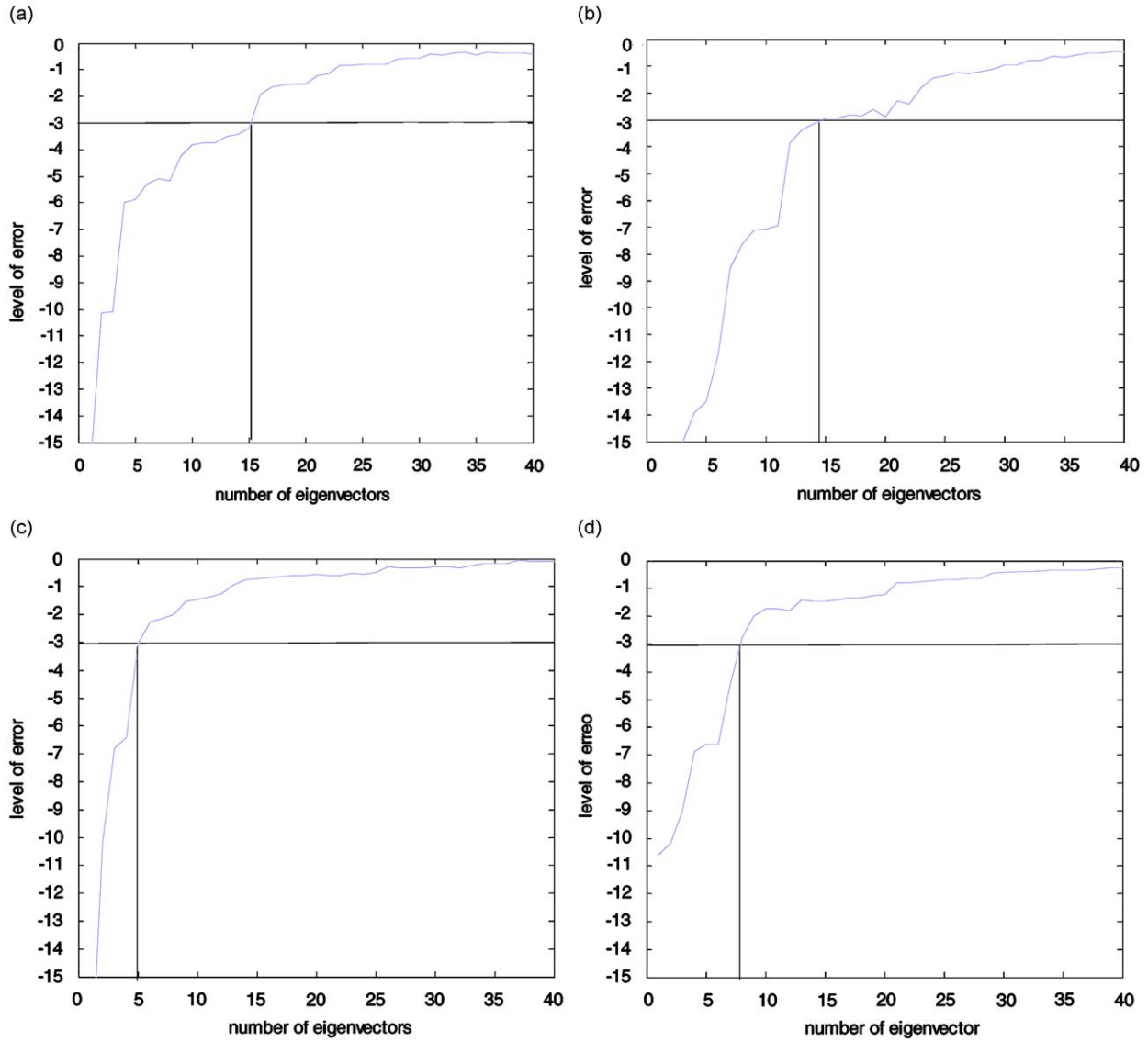

Fig. 17. Level of error on quadratic velocity, at different instants, versus size of the reduced model. Rectangular clamped aluminum plate excited at point (0.93, 0.35) by a unit impulse force filtered in the frequency band from 700 to 1551 Hz. Plate dimensions are: thickness 0.003, width 0.94, length 1.5. (a) t=0.032, (b) t=0.064, (c) t=0.128, and (d) t=0.516.

reduced model remains unchanged whatever the observation time after impulse excitation. As expected, the level of error on the quadratic velocity is greater when the size of the reduced model is smaller. It is generally admitted in practice that an error of 3 dB on the energy level is acceptable. With this criterion a reduced model with 15 dof is sufficient, which is a considerable reduction compared to standard modal decomposition in which at least 147 resonant modes must be considered.

7. Conclusion

In this paper we demonstrated that vibrations of systems of high modal density excited by broadband forces can be obtained by decomposing the response on a small number of effective shapes instead of using standard modal expansion. This result was explained by the phenomenon of mode grouping occurring in systems of high modal density. A presentation was given of an approach for building effective shapes from measured mobility matrices. This approach is of interest for systems with high modal density characteristic of mid and high frequency vibroacoustic problems. For the sake of robustness, energy is often preferred to local response for describing vibration behavior. In this case the number of effective shapes necessary for good precision is greatly reduced compared to the number of modes participating in the response. Applications of the method to plate vibration were presented and measured mobilities were used to build effective shapes and calculate the vibration velocity field and plate energy. Using the plate experiment data reported here, we observed that 15 effective shapes were sufficient to predict energy with an error less than 3 dB, in a frequency band in which 147 modes respond.

References

[1] R.J. Allemang, D.L. Brown, *Experimental Modal Analysis, Handbook on Experimental Mechanics*, VCH Publishers, 1993 pp. 635–750.
[2] J.R. Arruda, S.A. Do Rio, L.A. Santos, A space frequency data compression method for partially dense laser Doppler vibrometer and measurement, *Journal of Shock and Vibration* 3 (2) (1992) 127–133.
[3] S. Vanlanduit, P. Guillaume, J. Schoukens, Robust data reduction of high spatial resolution optical vibration measurements, *Journal of Sound and Vibration* 274 (1) (2004) 369–384.
[4] S. Vanlanduit, B. Caugerghe, P. Guillaume, P. Verboven, E. Parloo, Reduction of large frequency response functions data set using a robust singular value decomposition, *Computers and Structures* 84 (2006) 808–822.
[5] Y. Ren, C.F. Beards, On substructure synthesis with FRF data, *Journal of Sound and Vibration* 185 (5) (1995) 845–866.
[6] R.H. Lyon, G. Maidanik, Power flow between linearly coupled oscillators, *Journal of the Acoustical Society of America* 34 (1962) 623–639.
[7] R.H. Lyon, *Statistical Energy Analysis of Dynamical Systems: Theory and Applications*, M.I.T. Press, Cambridge, 1975.
[8] R.H. Lyon, R.G. DeJong, *Theory and Application of SEA*, Butterworth, London, 1995.
[9] R.S. Langley, A derivation of the coupling loss factors used in statistical energy analysis, *Journal of Sound and Vibration* 141 (2) (1990) 207–219.
[10] D.A. Bies, S. Hamid, In situ determination of loss and coupling loss factors by the power injection method, *Journal of Sound and Vibration* 70 (2) (1980) 187–204.
[11] L. Maxit, J.-L. Guyader, Estimation of SEA coupling loss factors using a dual formulation and FEM modal information, part 1: theory, *Journal of Sound and Vibration* 239 (5) (2001) 907–930.
[12] D. Karnopp, Coupled vibratory system analysis, using the dual formulation, *Journal of the Acoustical Society of America* 40 (1966) 380–384.
[13] B.R. Mace, J. Rosenberg, The SEA of two coupled plates: an investigation into effects of subsystem irregularity, *Journal of Sound and Vibration* 212 (3) (1998) 395–415.
[14] S. Finnveden, Ensemble average vibration energy flows in a three structural elements structure, *Journal of Sound and Vibration* 187 (3) (1995) 495–529.
[15] L. Maxit, J.-L. Guyader, Extension of SEA model to subsystems with non uniform modal energy distribution, *Journal of Sound and Vibration* 265 (2003) 337–358.
[16] N. Totaro, J.-L. Guyader, SEA substructuring using cluster analysis: the MIR index, *Journal of Sound and Vibration* 290 (2006) 264–289.
[17] G.J. O'Hara, Mechanical impedance and mobility concepts, *Journal of the Acoustical Society of America* 41 (1967) 1180–1184.
[18] R.J. Pinnington, R.G. White, Power flow through machine isolators to resonant and non resonant beams, *Journal of Sound and Vibration* 75 (2) (1981) 179–197.
[19] J.-M. Mondot, B.A.T. Peterson, Characterization of structure borne sound sources: the source descriptor and the coupling function, *Journal of Sound and Vibration* 114 (3) (1987) 264–289.
[20] B.A.T. Peterson, B.M. Gibbs, Toward a structure borne sound characterization, *Applied Acoustics* 61 (3) (2000) 325–343.
[21] A.T. Moorhouse, On the characteristic power of structure borne sources, *Journal of Sound and Vibration* 248 (3) (2001) 441–459.
[22] J.M. Cuschieri, Structural power flow analysis using a mobility approach of an L shaped plate, *Journal of the Acoustical Society of America* 87 (1990) 1159–1165.
[23] J.M. Cuschieri, Vibration transmission through periodic structures using a mobility power flow approach, *Journal of Sound and Vibration* 143 (1) (1990) 65–74.
[24] M. Ouisse, L. Maxit, C. Cacciolati, J.-L. Guyader, Patch transfer function as a tool to couple linear acoustic problems, *Journal of Vibration and Acoustics, ASME Transaction* 127 (2005) 458–466.
[25] G. Orefice, C. Cacciolati, J.-L. Guyader, The energy mobility, *Journal of Sound and Vibration* 254 (2) (2002) 269–295.
[26] C. Soize, Reduced models in the medium frequency range for general external structural acoustic systems, *Journal of the Acoustical Society of America* 103 (1998) 3393–3406.
[27] R. Ohayon, Reduced models for fluid structure excitation, *International Journal of Numerical Methods in Engineering* 60 (2004) 139–152.
[28] R. Ghanem, A. Sarkar, Reduced model for the medium-frequency dynamics of stochastic systems, *Journal of the Acoustical Society of America* 113 (2003) 834–846.
[29] J.-L. Guyader, Modal sampling method for the vibration study of systems of high modal density, *Journal of the Acoustical Society of America* 88 (1990) 2269–2276.
[30] J.-L. Guyader, *Vibrations in Continuous Media*, ISTE, London, 2006 441pp.